Normal state specific heat in the cuprate superconductors $La_{2-x}Sr_xCuO_4$ and $Bi_{2+y}Sr_{2-x-y}La_xCuO_{6+\delta}$ near the critical point of the pseudogap phase

C. Girod,[1,2] D. LeBoeuf,[3] A. Demuer,[3] G. Seyfarth,[3] S. Imajo,[4] K. Kindo,[4] Y. Kohama,[4] M. Lizaire,[2] A. Legros,[2] A. Gourgout,[2] H. Takagi,[5] T. Kurosawa,[6] M. Oda,[6] N. Momono,[7] J. Chang,[8] S. Ono,[9] G.-q. Zheng,[10,11] C. Marcenat,[12,*] L. Taillefer,[2,13,†] and T. Klein[1,‡]

[1]*Institut Néel, Université Grenoble Alpes, CNRS, Grenoble INP, F-38000 Grenoble, France*
[2]*Département de Physique, and RQMP, Institut Quantique, Université de Sherbrooke, Sherbrooke, Québec J1K 2R1, Canada*
[3]*Université Grenoble Alpes, INSA Toulouse, Université Toulouse Paul Sabatier, EMFL, CNRS, LNCMI, F-38000 Grenoble, France*
[4]*Institute for Solid State Physics, University of Tokyo, Kashiwa, Chiba 277-8581, Japan*
[5]*Department of Advanced Materials, University of Tokyo, Kashiwa 277-8561, Japan*
[6]*Department of Physics, Hokkaido University, Sapporo 060-0810, Japan*
[7]*Muroran Institute of Technology, Muroran 050-8585, Japan*
[8]*Physik-Institut, Universitat Zurich, Winterthurerstrasse 190, CH-8057 Zurich, Switzerland*
[9]*Central Research Institute of Electric Power Industry, Materials Science Research Laboratory, 2-6-1 Nagasaka, Yokosuka, Kanagawa, Japan*
[10]*Department of Physics, Okayama University, Okayama 700-8530, Japan*
[11]*Institute of Physics, Chinese Academy of Sciences, Beijing National Laboratory for Condensed Matter Physics, Beijing 100190, China*
[12]*Université Grenoble Alpes, CEA, Grenoble INP, IRIG, PHELIQS, 38000 Grenoble, France*
[13]*Canadian Institute for Advanced Research, Toronto, Ontario M5G 1M1, Canada*

(Received 20 January 2021; revised 14 May 2021; accepted 14 May 2021; published 7 June 2021)

The specific heat C of the cuprate superconductors $La_{2-x}Sr_xCuO_4$ and $Bi_{2+y}Sr_{2-x-y}La_xCuO_{6+\delta}$ was measured at low temperatures (down to 0.5 K) for dopings p close to $p^\star$, the critical doping for the onset of the pseudogap phase. A magnetic field up to 35 T was applied to suppress superconductivity, giving direct access to the normal state at low temperatures, and enabling a determination of C_e, the electronic contribution to the normal-state specific heat at $T \to 0$. In $La_{2-x}Sr_xCuO_4$ at $x = p = 0.22$, 0.24 and 0.25, $C_e/T = 15$ to 16 mJ mol^{-1} K^{-2} at $T = 2$ K, values that are twice as large as those measured at higher doping ($p > 0.3$) and lower doping ($p < 0.15$). This confirms the presence of a broad peak in the doping dependence of C_e at $p^\star \simeq 0.19$ as previously reported for samples in which superconductivity was destroyed by Zn impurities. Moreover, at those three dopings, we find a logarithmic growth as $T \to 0$ such that $C_e/T \sim B \ln(T_0/T)$. The peak versus p and the logarithmic dependence versus T are the two typical thermodynamic signatures of quantum criticality. In the very different cuprate $Bi_{2+y}Sr_{2-x-y}La_xCuO_{6+\delta}$, we again find that $C_e/T \sim B \ln(T_0/T)$ at $p \simeq p^\star$, strong evidence that this $\ln(1/T)$ dependence of the electronic specific heat—first discovered in the cuprates $La_{1.8-x}Eu_{0.2}Sr_xCuO_4$ and $La_{1.6-x}Nd_{0.4}Sr_xCuO_4$—is a universal property of the pseudogap critical point.

DOI: 10.1103/PhysRevB.103.214506

I. INTRODUCTION

Unraveling the mystery of high-temperature superconductivity remains a fundamental issue in modern solid-state physics. A central question is the nature of the enigmatic pseudogap phase which appears below a temperature $T^\star$ and a critical hole concentration (doping) $p^\star$. Well above $p^\star$, the Fermi surface consists of a large quasi-two-dimensional (2D) cylinder (see, for instance, Refs. [1,2] in $Tl_2Ba_2CuO_{6+\delta}$), the measured carrier concentration is equal to $n_H = 1 + p$ (per CuO_2 plane), and the Sommerfeld coefficient is on the order of 5 mJ mol^{-1} K^{-2} [3–6]. On the other hand, for $p \leqslant p^\star$, angle-resolved photoemission spectroscopy (ARPES) studies show that the Fermi surface breaks into small nodal "Fermi arcs" [7] and Hall effect measurements then indicate that the carrier concentration drops to $n_H = p$ in $YBa_2Cu_3O_y$ (YBCO) [8], $Nd_{0.4}La_{1.6-x}Sr_xCuO_4$ (Nd-LSCO) [9], and $Bi_{2+y}Sr_{2-x-y}La_xCuO_{6+\delta}$ (Bi2201) [10,11].

Specific-heat measurements in the normal state of Nd-LSCO and $Eu_{0.2}La_{1.8-x}Sr_xCuO_4$ (Eu-LSCO) [4] recently showed that the electronic contribution to the specific heat C_e/T, actually displays a pronounced peak as function of doping at $p \sim p^\star$. Moreover, for p close to $p^\star$, the electronic specific heat displays a logarithmic temperature dependence: $C_e/T = B \ln(T_0/T)$ [4]. Both behaviors are typical thermodynamic signatures of quantum criticality [12]. It is important to investigate whether these characteristic features are also present—or not—in other cuprates. We, hence, report here a study of the temperature and doping dependence of the electronic specific heat C_e in $La_{2-x}Sr_xCuO_4$ (LSCO) and Bi2201 single crystals.

*christophe.marcenat@cea.fr
†louis.taillefer@usherbrooke.ca
‡thierry.klein@neel.cnrs.fr

In LSCO, large C_e/T values (on the order of 15 mJ mol^{-1}K^{-2} at 2 K) are measured in the vicinity of the onset of the pseudogap phase. However, in contrast to previous measurements in Nd/Eu-LSCO [4], C_e/T remains large over an extended doping range, confirming the former indication for the presence of a *broad* maximum in the doping dependence of C_e/T observed in Zn-substituted samples [13]. Despite the presence of a large (hyperfine) Schottky contribution, we also show that a $B\ \ln(T_0/T)$ contribution has to be introduced in order to fit the temperature dependence of C_e/T. Similarly, a clear $B\ \ln(T_0/T)$ contribution to C_e/T and concomitant large C_e/T values (on the order of 13 mJ mol^{-1}K^{-2} at 0.65 K) are observed in Bi2201 for $p \sim p^\star$, hence, confirming the universality of these features. Very similar values of the B coefficient are observed in all compounds (close to $p^\star$) and the influence of the magnetic field on T_0 will be discussed.

II. METHODS

The specific heat of seven LSCO single crystals with $0 \leqslant p \leqslant 0.25$ and four Bi2201 single crystals with doping contents close to the onset of the pseudogap phase has been measured by AC microcalorimetry in a ^{3}He system down to about 0.5 K and up to 35 T. Unless otherwise indicated all the magnetic fields used in this paper were static. Sample LSCO No. 3 and LSCO No. 4 are the same samples than measured in Refs. [14,15]. A transport study of sample Bi2201 No. 1 and Bi2201 No. 4 (labeled OD10K and OD18K, respectively) has recently been performed in Ref. [11]. The temperature T^* was determined from the temperature dependence of the Knight shift for Bi2201 No. 2 and No. 3 [16].

The heat capacity was measured by a modulation technique where a periodically modulated heating power P_{AC} is applied at a frequency 2ω. Recording the amplitude of the induced temperature oscillations $|T_{AC}|$ and its thermal phase shift ϕ relative to the power allows to calculate the heat capacity: $C_p = P_{AC}\sin(-\phi)/2\omega|T_{AC}|$. A miniature CERNOX resistive chip has been split into two parts and attached to a small copper ring with PtW(7%) wires. The first half (R_H) was then used as an electrical heater [$P_{AC} = R_H i_{AC}^2(\omega)/2$] and the second ($R_T$) was used to record the temperature oscillations [$V_{AC}(2\omega) = (dR_T/dT)T_{AC}(2\omega)i_{DC}$, where i_{DC} is a DC reading current]. In order to subtract the heat capacity of the addenda (chip + a few milligrams of Apiezon grease used to glue the sample onto the back of the chip), the empty chip was measured prior to the sample measurements. A precise *in situ* calibration and corrections of the thermometers in the magnetic field were included in the data treatment. This technique enabled us to obtain absolute values of the heat capacity of minute single crystals with an absolute accuracy better than ~95% as deduced from measurements on ultra pure copper (for further details, see Ref. [4]).

Sample Bi2201 No. 2 was also measured in pulsed magnetic fields up to 39 T and down to 0.6 K by the heat pulse method described in Ref. [17]. The single crystal was mounted on the sample platform with a small amount of Apiezon grease, and the total heat capacity was estimated by $C_p = Q/\Delta T$, where Q is the applied heat and ΔT is the resultant temperature change. The addenda contribution originating from the sample platform and Apiezon grease was estimated by a separate experiment. The thermometer was calibrated by isothermal measurements of the magnetoresistance, and the accuracy of C_p was estimated to ~93% below 2 K and ~90% between 2 and 4 K as deduced from measurements on a reference sample of polycrystalline Ge [17].

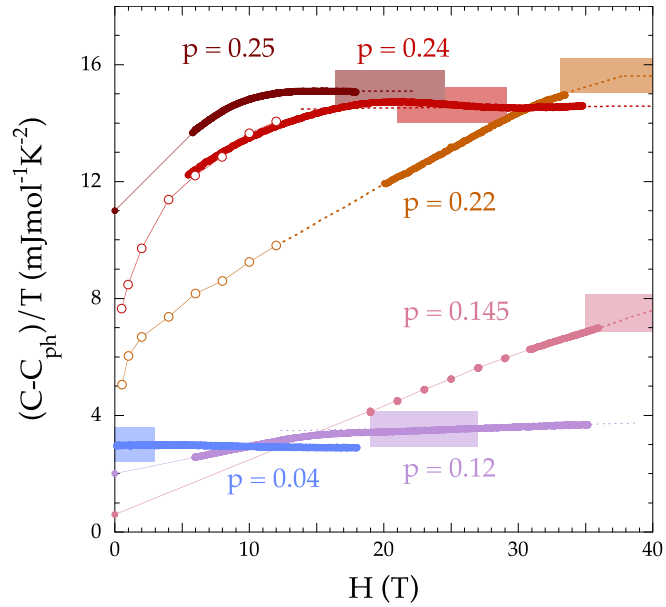

FIG. 1. Magnetic-field dependence of the specific heat at $T \sim 2$ K in $La_{2-x}Sr_xCuO_4$ (sample details are shown in Table I) after subtraction of the phonon contribution C_{ph} (see Fig. 3). The small overshoot observed for $p \sim 0.24$ is most probably reminiscent of the superconducting transition in presence of strong fluctuations. The shaded (colored) boxes indicate the locus of the previously estimated $H_{c2}(0)$ values [14,18]. Open circles are low-field data extracted from Ref. [6]. As seen, $(C - C_{ph})/T$ increases with p, reaching ~15 to 16 mJ mol^{-1} K^{-2} in the normal state for $p \sim 0.22$–0.25 (see also Fig. 2).

III. RESULTS AND DISCUSSION

A. $La_{2-x}Sr_xCuO_4$

Efforts to measure the normal state specific heat at low temperatures in LSCO have been hindered by the very large upper critical-field values exceeding 60 T around optimal doping (for $0.14 \leqslant p \leqslant 0.21$ [18], see also Ref. [14] and references therein). This implies that measurements in the normal state have been limited to highly underdoped or overdoped samples in which superconductivity is absent [5,6,19] or weak enough to be easily suppressed by moderate magnetic fields [6,18]. However, ARPES measurements indicated that the pseudogap critical point $0.17 \leqslant p^\star \leqslant 0.22$ [20,21]. Accordingly, resistivity measurements suggested that $p^\star = 0.19 \pm 0.02$ [22–24], i.e., lying in the doping range for which the normal state is unattainable.

As shown in Fig. 1, the specific heat increases with the magnetic field in the mixed state and saturates at high fields, clearly indicating that the applied fields are large enough to suppress superconductivity [or are slightly below $H_{c2}(0)$ for $p \sim 0.22$ and 0.145]. The field values above which C/T

saturates (at 2 K) are in very reasonable agreement with the $H_{c2}(0)$ values inferred from transport measurements [14,18] [shaded (colored) boxes in Fig. 1]. Similarly, the field-induced softening in sound velocity measurements and the field dependence of $1/T_1$ in NMR measurements both stop at about 40 T at 4 K for $p \sim 0.21$ [14] which is again consistent with our estimated $H_{c2}(0)$ values. Moreover, at higher temperatures, the crossover from the superconducting to the normal state shows up as a broad maximum in the field—and/or temperature—dependence of C/T (see the Supplemental Material [25]). This smeared maximum (still visible at 2 K in Fig. 1 for $p \sim 0.24$) is then reminiscent of the former specific jump at H_{c2}, indicating the locus in the H-T phase diagram where most of the change in the superconducting ordering energy occurs. All measurements were performed above this bump. Finally, we stress that the Wiedemann-Franz law is obeyed in Nd-LSCO $p \sim 0.24$ at a field of 10 T (and above) [26], showing that above 10 T there is no trace of superconductivity, in good agreement with the field above which the specific heat saturates [4]. By applying magnetic fields up to 35 T, we were, hence, able to determine the specific heat in the normal state for p values as close as possible to $p^\star$.

Note that a H^2 field dependence is observed at the lowest temperatures for $H \geqslant H_{c2}(0)$, indicating the presence of a hyperfine Schottky contribution: $C_{\rm hyp} = AH^2/T^2$ with $A \sim 4 \pm 1 \times 10^{-3}$ mJ mol^{-1} K^{-1} T^{-2} (see the Supplemental Material [25] and Fig. 3 below). This hyperfine term is unfortunately hindering any unambiguous determination of the electronic contribution at very low temperatures, and we have here limited our lowest temperature to ~2 K for the analysis of C_e/T as $C_{\rm hyp}/T$ becomes negligible above this temperature (see Fig. 5 in the Supplemental Material [25] for the relative contribution of each term).

Our measurements then clearly indicate that the normal state electronic contribution to the specific heat displays a maximum upon doping [see Fig. 2(a)], similar to the one observed in Nd- and Eu-substituted LSCO [4] [Fig. 2(b)]. As shown, very similar C_e/T values are obtained for $p \geqslant 0.25$, but clear differences are visible for lower dopings. Indeed, the position of the peak is shifted towards lower dopings in LSCO compared to its Nd- and Eu-substituted counterparts, due to the lower $p^\star$ value. However, the maximum is significantly broader in LSCO, in agreement with the doping dependence of the electronic specific heat previously obtained in Zn-substituted samples [13] [see Fig. 2(c)]. Even though there exists some uncertainty on the determination of p, it is worth noting that those large C_e/T values have been observed in samples with upper critical fields ranging from $H_{c2} \sim 14$ T to $H_{c2} \geqslant 34$ T (see Fig. 1), unambiguously confirming that C_e/T remains large over an extended doping range (from $p \approx 0.20$ to $p \approx 0.26$).

Note that attempts to determine the electronic contribution from high-temperature specific-heat measurements (i.e., for $T > T_c$) led to inconclusive results close to p^*. Those determinations were based on a difficult phonon subtraction procedure, and reported values vary from 7 [27] to 14 mJ mol^{-1} K^{-2} [28]. The latter value seems to be consistent with our paper (see Fig. 2), but C_e/T actually decreases with T, hindering any direct comparison between those high-temperature values and those obtained here for $T \to 0$.

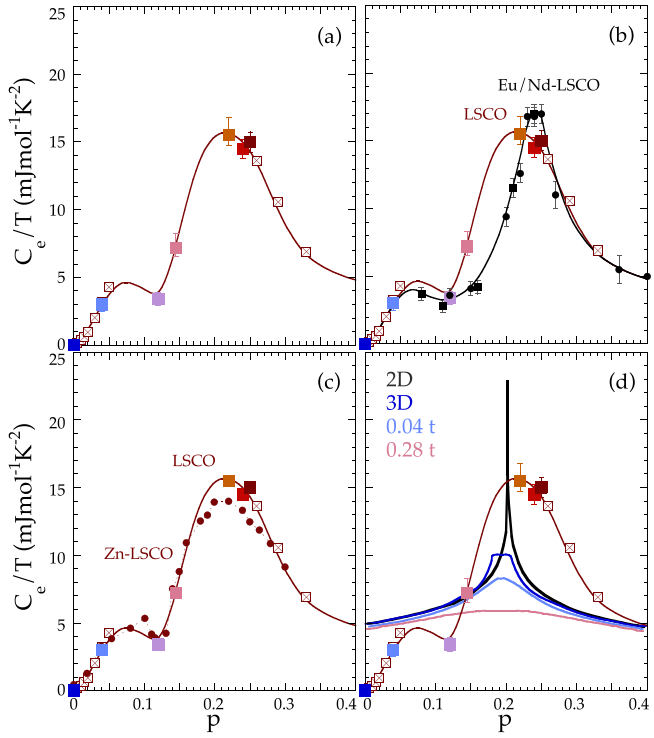

FIG. 2. (a) Electronic contribution to the specific heat C_e/T (at 2 K) as a function of the doping content p in $La_{2-x}Sr_xCuO_4$ (solid squares, see Table I for sample details) together with data previously obtained in samples of lower H_{c2} values [5,6,19] (crossed open squares). The same guide to the eye (thin line) is used in all panels. (b) The same data as panel (a) together with data previously obtained in Nd-LSCO (black circles) and LSCO (black squares) crystals (from Ref. [4]). (c) The same data as in panel (a) together with data previously obtained in samples in which superconductivity was destroyed by Zn impurities [13] [(red) closed circles]. (d) The same data as in panel (a) together with calculations from Ref. [29] for a van Hove singularity at $p_{\rm vHs} = 0.2$ (solid lines) for the indicated geometries [2D/three dimensional (3D)] and scattering rates ($\hbar/\tau$, see Ref. [29] for details). As shown, the dependence obtained for any van Hove singularity only very poorly reproduces the experimental data.

The change in topology of the Fermi surface at $p_{\rm vHs} \gtrsim p^\star$ is expected to give rise to a strong (diverging) van Hove singularity in a purely 2D system [29] [see the black line in Fig. 2(d)]. In fact, the amplitude of this singularity is strongly reduced both by the non-zero dispersion along k_z and the presence of disorder. The dark-blue line in Fig. 2(d) is a calculation of its contribution to the specific heat for an anisotropic 3D system with a transverse hopping rate $t_z = 0.07t$, t being the nearest-neighbor hopping parameter in the tight-binding Hamiltonian. The light-blue and purple lines are calculations for scattering rates τ equal to $\hbar/\tau = 0.04t$ and $0.28t$, respectively [29] (the latter value is consistent with the measured residual resistivity $\rho_0 \sim 30\ \mu\Omega$ cm). We deduce from Fig. 2(d) that the computations poorly reproduce the experimental data. Moreover, as disorder is very different in pristine LSCO- and Zn-substituted samples, one should have observed a much reduced peak in the latter. This is not the case, hence, strongly suggesting that the observed peak is not related to this van Hove singularity.

Finally, it is interesting to compare our data on LSCO at $p = 0.04$ with recent quantum oscillation measurements in the five-layer cuprate $Ba_2Ca_4Cu_5O_{10}(F, O)_2$ [30]. The frequency of the oscillations coming from the innermost layer (labeled IP0) in which there is long-range antiferromagnetic order is $F = 147$ T. ARPES measurements show that the Fermi surface in this metal with antiferromagnetic order consists of four small closed hole pockets at nodal locations in the Brillouin zone, centered approximately at $(\pm\pi/2, \pm\pi/2)$ [30]. The 2D carrier density n contained by each hole pocket is given by $n = F/\Phi_0$, where $\Phi_0 = h/2e$. The hole concentration (doping) p should then be given by $p = 2n$, given that there are two hole pockets per magnetic Brillouin zone, which yields $p \simeq 0.04$. The effective mass extracted from the quantum oscillations is $m^* \sim 0.7m_e$, where m_e is the bare electron mass. This corresponds to a specific-heat Sommerfeld coefficient $\gamma = 2 \times 1.43m^* \sim 2$ mJ mol^{-1} K^{-2} mol^{-1} Cu^{-1} where the factor 2 comes from having two hole pockets in the Brillouin zone. This expected value of γ is not far from the value of 3 mJ mol^{-1} K^{-2} mol^{-1} Cu^{-1} reported here for LSCO at $p = 0.04$ (Figs. 1 and 2). Given that the carrier density estimated from the Hall number in LSCO at $p = 0.04$ is indeed $n = n_H \simeq 0.04$ [31], the Fermi surface of LSCO at $p = 0.04$ should be the same as that observed on the inner plane of $Ba_2Ca_4Cu_5O_{10}(F, O)_2$, i.e., four nodal hole pockets containing p carriers, even though the commensurate antiferromagnetic phase in LSCO ends at $p \simeq 0.02$. This points to a similar Fermi surface in the pseudogap phase, beyond $p \simeq 0.02$, and in the antiferromagnetic phase as suggested by Hall studies in various cuprates [8,9,11] and associated calculations [32–35].

Another indication for the presence of a quantum critical point (QCP) is the occurrence of a $\ln(1/T)$ contribution in the temperature dependence of the specific heat [4,12]. As shown in Fig. 3, the data can be well described by the standard $C/T = \gamma_0 + \beta T^2$ law above ~2 K for dopings far from the critical doping $p^\star$, i.e., for $p \leqslant 0.145$ and $p \geqslant 0.29$ (a small δT^4 correction has to be introduced above ~5 K). At very low temperatures, a clear deviation due to the hyperfine contribution is visible, in good agreement with the H^2 dependence observed in $C/T(H)$ (see Fig. 2 in the Supplemental Material [25]). In contrast with data at $p = 0.12$, the upturn at low temperatures cannot be described by the hyperfine contribution alone for dopings close to $p^\star$ (i.e., for $p \sim 0.22$–0.25), indicating an extra contribution which extends well above 2 K. Note that a very similar contribution is also visible in the data previously obtained by Wang *et al.* [6] for $p = 0.26$ (see Fig. 1 in the Supplemental Material [25]). Such an upturn has also been observed in Zn-LSCO (below ~3.5 K) and has been attributed to local magnetic moments induced by Zn doping [13], but this interpretation cannot hold in our pristine LSCO crystals.

In this doping range, the data can then be very well fitted by introducing an extra $\ln(1/T)$ contribution to the specific-heat $C/T = AH^2/T^3 + \beta T^2 + \delta T^4 + B\ln(T_0/T)$ (see solid lines in Fig. 3) where the constant $B\ln(T_0)$ term contains both the band-structure Sommerfeld contribution and a cutoff temperature above which the contribution of the (quantum) fluctuations vanishes. To clearly highlight this logarithmic contribution, it is displayed in Fig. 3(a) as a shaded area under the curve for $p = 0.25$. On the contrary, a very good fit to the data can be obtained with $B = 0$ for $p = 0.12$ [see the dashed line in Fig. 3(b)]. Note that a $\ln(1/T)$ contribution to microwave resistivity measurements has been reported by Zhou *et al.* [36] in YBCO and $Tl_2Ba_2CuO_{6+\delta}$. This logarithmic upturn has been attributed to flux flow resistivity in the mixed state of d-wave superconductors, but such an explanation cannot account for our specific-heat measurements which were carried out in the normal state (see Fig. 1 and the discussion above).

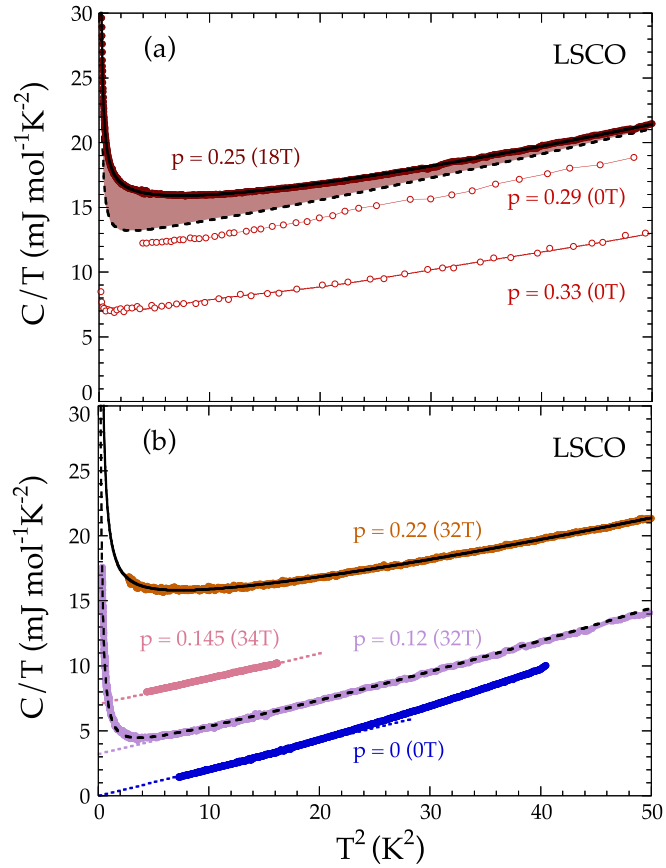

FIG. 3. Temperature dependence of the specific heat obtained in $La_{2-x}Sr_xCuO_4$ for $p \geqslant 0.25$ [panel (a)] and $p \leqslant 0.22$ [panel (b)] at the indicated magnetic fields (see Table I for sample details). For $p = 0.22$ and 0.25, the data can be well described by $C/T = AH^2/T^3 + \beta T^2 + \delta T^4 + B\ln(T_0/T)$ [(black) solid lines]. The (black) dashed line in panel (a) corresponds to the dependence that would be obtained for $B = 0$ ($p \sim 0.25$), and the shaded area then highlights the contribution of the $B\ln(T_0/T)$ term. By contrast, a good fit to the data can be obtained with $B = 0$ for $p = 0.12$ [(black) dashed line in panel (b)]. The standard $C/T = \gamma_0 + \beta T^2$ dependence is indicated by the dotted lines [panel (b)]. As seen for $p \sim 0.12$, the hyperfine (AH^2/T^3) contribution becomes negligible above 3 K. The data at $p = 0.29$ and $p = 0.33$ (open symbols) are from Refs. [5,6], respectively (see also the Supplemental Material for other compositions [25]).

B. $Bi_{2+y}Sr_{2-x-y}La_xCuO_{6+\delta}$

We performed similar measurements on four Bi2201 crystals (see Table I). It is difficult to determine an unambiguous

TABLE I. Sample name, critical temperature T_c, chemical substitution rates (x and y), estimated $T = 0$ upper critical field (* from Refs. [14,18]), sample mass, and B coefficient in the $B\ln(T_0/T)$ contribution to the specific heat of the $Bi_{2+y}Sr_{2-x-y}La_xCuO_{6+\delta}$ and $La_{2-x}Sr_xCuO_4$ single crystals. Bi2201 samples No. 1 and No. 4 are the same as OD10K and OD18K in Ref. [11], respectively. Bi2201 samples No. 2 and No. 3 are the same as those for which the NMR Knight shift was reported in Ref. [16], yielding estimates of the pseudogap temperature $T^\star$ as plotted in Fig. 6. Last line: Data from Ref. [4].

Name	T_c (K)	x	y	$H_{c2}(0)$ (T)	Mass (mg)	B (mJ mol^{-1} K^{-2})
Bi2201 No. 1	∼11.5	0	0.05	∼15	0.42	2.8 ± 0.5
Bi2201 No. 2	∼10	0.04	0	∼15	1.20	3.2 ± 0.5
Bi2201 No. 3	∼13.5	0.08	0	∼17	0.37	2.5 ± 0.5
Bi2201 No. 4	∼18	0.20	0	∼22 (at 2.1 K)	0.39	<1
LSCO No. 1	0	0		0	0.60	0
LSCO No. 2	0	0.04		0	0.95	0
LSCO No. 3	∼20	0.12		∼19	0.75	0
LSCO No. 4	∼25	0.145		$40 \pm 5^*$	1.50	0
LSCO No. 5	∼25	0.22		$37 \pm 4^*$	0.94	2.0 ± 0.3
LSCO No. 6	∼16	0.24		∼23 (at 2.1 K)	1.50	2.2 ± 0.3
LSCO No. 7	∼15	0.25		∼14 (at 2.1 K)	0.85	2.1 ± 0.3
Eu-LSCO	11	$p = 0.24$		11		2.5 ± 0.5

doping content p in $Bi_{2+y}Sr_{2-x-y}La_xCuO_{6+\delta}$ due to the various doping routes (x, y, and δ). The phase diagram is then usually plotted as a function of the critical temperature T_c (see Fig. 6 below) and the onset of the pseudogap phase—as deduced from ARPES [37] and NMR [38] studies—occurs in the highly overdoped regime for $T_c \sim 8$ K. All measurements were, hence, performed within the pseudogap phase, with $p \sim p^\star$ in Bi2201 No. 2.

As shown in Fig. 4, the electronic specific heat is on the order of 8 ± 1 mJ mol^{-1} K^{-2} at 3 K but rapidly increases with decreasing temperature, reaching $\sim 13 \pm 1$ mJ mol^{-1} K^{-2} at 0.65 K in Bi2201 Nos. 1–3. In Bi2201, the hyperfine contribution to the specific heat we observe is much weaker than in LSCO ($A = 8 \pm 1 \times 10^{-4}$ mJ mol^{-1} K^{-1} T^{-2}), and the normal state could be reached in all measured samples [see Table I and Fig. 4 in the Supplemental Material [25] for the upper critical field $H_{c2}(0)$ values]. As an example, in the normal state of sample Bi2201 No. 1 at a field just above $H_{c2}(0) \sim 15$ T, the hyperfine term is about 20 times smaller than in LSCO. The contribution of the $\ln(1/T)$ term can then be straightforwardly identified in the temperature dependence of C/T and is highlighted by a shaded area in Fig. 4(a) (see Fig. 5 in the Supplemental Material [25] for the relative contribution of each term).

Complementary measurements have also been performed in Bi2201 No. 2 in pulsed magnetic fields up to ∼39 T [see Fig. 4(b)]. Although slightly larger, the obtained C/T values are in reasonable agreement with the one obtained in DC field. They confirm the presence of a clear upturn at low temperatures and the absence of any significant contribution from the hyperfine term (i.e., no field dependence) up to 39 T on the whole temperature range. In all samples, C/T can then be very well fitted by a $AH^2/T^3 + \beta T^2 + B\ln(T_0/T)$ law (solid lines in Fig. 4). In samples Bi2201 Nos. 1–3, the amplitude of the logarithmic contribution is identical within error bars (see Table I) and this contribution is only significantly smaller in Bi2201 No. 4, which has the highest T_c and, hence, a doping content further away from $p^\star$ [see the shaded area in Fig. 4(d)].

It is worth noting that we obtained very similar B coefficients (∼2 to 3 mJ mol^{-1} K^{-2} close to $p^\star$) in LSCO, Nd/Eu-LSCO, and Bi2201 (see Table I). Following Varma [39],

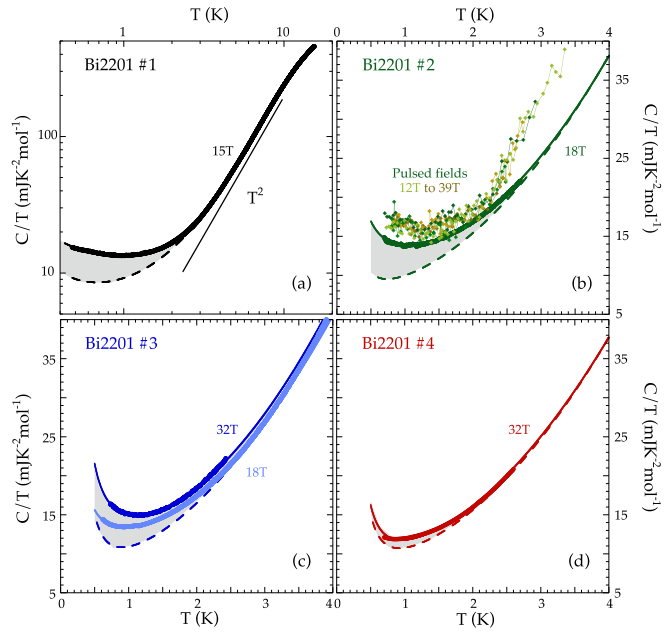

FIG. 4. Temperature dependence of the specific heat of our $Bi_{2+y}Sr_{2-x-y}La_xCuO_{6+\delta}$ single crystals (see Table I for sample details). Solid lines are fit to the data assuming that $C/T = AH^2/T^3 + \beta T^2 + B\ln(T_0/T)$, and the dashed line corresponds to the dependence that would be obtained for $B = 0$. The contribution of the $B\ln(T_0/T)$ term is highlighted by the gray shaded area. As shown in panel (d), the contribution of the $\ln(1/T)$ term is much weaker in Bi2201 No. 4 which has a larger T_c value. Complementary pulsed field data in our Bi2201 No. 2 sample for fields ranging from 12 to 39 T are also displayed in panel (b). Measurements of Bi2201 No. 3 at both 18 and 32 T are displayed in panel (c), indicating a field dependence of C/T in the normal state, well above 1 K (see also Fig. 6 and text for the details).

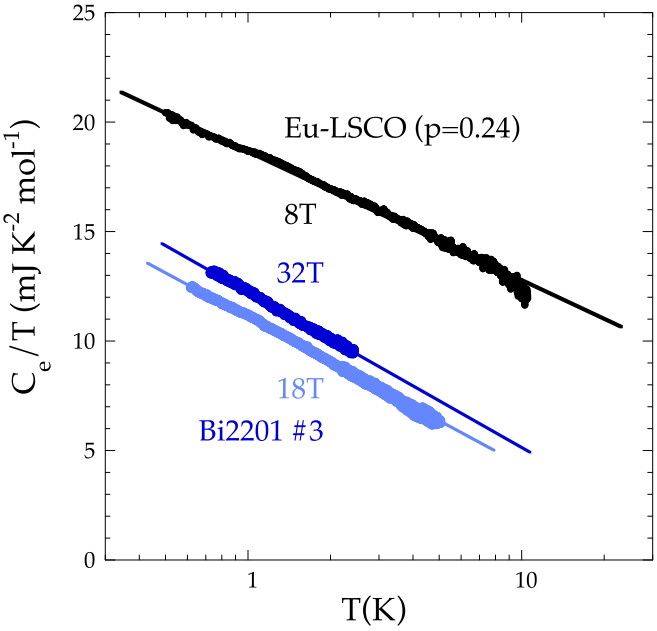

FIG. 5. Temperature dependence of the electronic contribution to the specific heat $C_e/T = C/T - AH^2/T^3 - C_{ph}/T$ of Bi2201 No. 3, compared to the dependence previously obtained in Eu-LSCO in Ref. [4], clearly displaying the logarithmic temperature dependence [$C_e/T = B\ \ln(T_0/T)$] with a field-dependent $T_0(H)$.

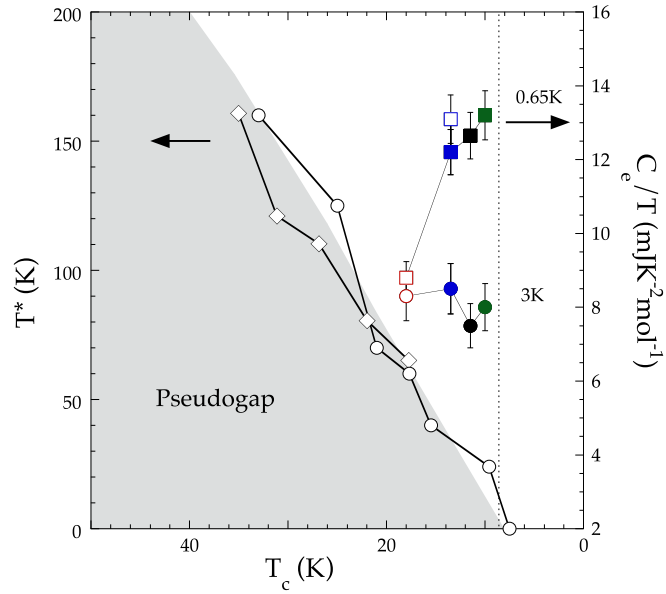

FIG. 6. Electronic specific heat C_e/T as a function of the critical temperature T_c at 0.65 K (squares) and 3 K (circles) for Bi2201 samples No. 1 (black), No. 2 (green), No. 3 (blue), and No. 4 (red) (same color code as in Fig. 4), together with the evolution of the pseudogap phase onset temperature $T^\star$ as deduced from ARPES (diamonds from Ref. [37]) and NMR (circles from Refs. [16,38]) measurements. Closed symbols correspond to 18-T measurements and open symbols to 32-T measurements, suggesting a (small) increase of the electronic contribution with field in the normal state (see Fig. 5).

B is expected to be on the order of the band-structure Sommerfeld coefficient γ_0 and our B value is then *quantitatively* consistent with a γ_0 value being on the order of 5 mJ mol^{-1} K^{-2} as measured far from $p^\star$ (the coupling constant $g = B/\gamma_0 \sim 0.5$ is in agreement with transport and photoemission measurements, see Ref. [39] for a detailed discussion). This $B \sim \gamma_0$ scaling also well agrees with the fact that much larger B values were reported in heavy fermions (~500 mJ mol^{-1} K^{-2} [40]).

On the other hand, $B\ln(T_0)$ varies from ~11 to 12 mJ mol^{-1} K^{-2} in Bi2201 to ~16–19 mJ mol^{-1} K^{-2} in lanthanum-based cuprates (see Fig. 5). This increase in T_0 is consistent with Seebeck coefficient measurements [11,41,42] showing that, at low temperatures, $S(T)$ is significantly larger in Nd/Eu-LSCO than in Bi2201. $S(T)$ also displays a $\ln(1/T)$ temperature dependence, but this contribution is then flattening off above ~30 K in Bi2201 whereas it extends up to ~100 K in Nd/Eu-LSCO. Finally, note that we observe a small increase in T_0 with field in Bi2201 No. 3 [see Figs. 4(c) and 5]. Although small, this field-induced change cannot be attributed to the Schottky contribution (see Fig. 6 in the Supplemental Material [25]) and still has to be understood (see also concluding remarks below).

Finally, let us turn to the doping dependence of C_e/T in Bi2201. As shown in Fig. 6, the electronic specific heat is on the order of 8 ± 1 mJ mol^{-1} K^{-2} at 3 K but rapidly increases with decreasing temperature, reaching ~13 ± 1 mJ mol^{-1} K^{-2} at 0.65 K in Bi2201 Nos. 1–3. As shown, C_e/T at 0.65 K then decreases in Bi2201 No. 4. Bi2201 Nos. 1–3 clearly lie close to the onset of the pseudogap phase, emphasizing the enhancement of C_e/T (at low T) in the vicinity of this point. Note that a linear temperature dependence of the resistivity has been reported recently in Bi2201 No. 1 (labeled OD10K) [11] but this linearity does not persist down to $T = 0$ K, indicating that the doping content is slightly below $p^\star$ for this T_c value.

It is interesting to further compare our specific-heat data on Bi2201 with recent transport measurements performed on the same samples (samples labeled OD10K and OD18K in Ref. [11] are the same as Bi2201 No. 1 and Bi2201 No. 4, respectively). In particular, the Hall effect measurements yield a large difference in Hall number between the two, namely, $n_H \sim 1.4$ for Bi2201 No. 1 and $n_H \sim 0.75$ for Bi2201 No. 4, interpreted as a sharp nearly twofold drop in carrier density with decreasing p [11]. A similar decrease has been reported by Putzke *et al.* [10] and a very similar drop was observed previously in YBCO [8] and Nd-LSCO [9]. This drop has been identified as a key signature of the pseudogap phase that reveals a transformation of the Fermi surface across $p^\star$, consistent with a change from a large surface containing $1 + p$ holes to small Fermi pockets containing p holes [32,43]. Note that for the same Bi2201 samples, the electronic specific heat at $T = 3$ K changes very little from one doping to the other (Fig. 6). This is not necessarily incompatible with a transformation of the Fermi surface. Indeed, calculations show that when a metal undergoes a transition into a phase of antiferromagnetic order (at $T \simeq 0$) [34], the specific heat is barely affected initially whereas the Hall number exhibits a rapid drop.

Another property of Bi2201 that was measured in the field-induced normal state at $T \to 0$ is the NMR Knight shift

[38], which reflects the electronic spin susceptibility, typically assumed to be proportional to the electronic density of states. In that sense, it should be closely related to the electronic specific heat reported here. What we observe is that the two quantities do not show the same degree of change below $p^\star$. Indeed, although the electronic spin susceptibility at $T \simeq 2$ to 3 K drops by a factor of about 20% in going from $T_c = 10$ to $T_c = 18$ K [38], the electronic specific heat does not change (Fig. 6). This suggests that the two measurements, performed in the very same conditions of temperature and field, on the same Bi2201 samples, do not reflect the same underlying physical quantity, i.e., they do not both reflect the same density of states. Understanding this difference, revealed here for the first time in a cuprate material, should provide new insight into the nature of the pseudogap phase.

IV. CONCLUDING REMARKS

To summarize, we have shown that the electronic contribution to the normal state specific heat displays a $\ln(1/T)$ temperature dependence associated with a strong increase in C_e/T for $T \to 0$, close to the critical doping $p^\star$ that marks the onset of the pseudogap phase in both LSCO and Bi2201 as previously observed in Nd/Eu-LSCO [4]. These features seem, therefore, generic in cuprates and are classical signatures of the existence of a QCP, whose nature has not yet been identified. In LSCO, the $\ln(1/T)$ term is observed, at least, up to $p = 0.26$, i.e., well above $p^\star = 0.19 \pm 0.02$. This extended doping range could be reminiscent of the *anomalous* form of criticality previously pointed out by Cooper *et al.* in transport measurements [24] for which a linear term in the temperature dependence of the resistivity is observed from $p \sim 0.18$ up to $p \sim 0.3$.

Moreover, we observed that the criticality is reinforced by the magnetic field in Bi2201 (the large hyperfine contribution and H_{c2} values are hindering a similar study in LSCO) as the electronic contribution to the specific heat slightly increases with field in the normal state. This puzzling behavior is in contrast to the one usually observed in heavy fermion systems in the vicinity of a magnetic QCP [12]. Indeed, in this case the quantum fluctuations are suppressed by the application of magnetic field, and the $\ln(1/T)$ contribution saturates at low temperature for large field values. Recent NMR and sound velocity measurements [14] indicated that the short-range magnetism is reinforced under high magnetic fields in LSCO. The interplay between this magnetic state and the signatures of quantum criticality observed here still has to be clarified, but it is worth noting that this magnetic phase vanishes at a critical doping which extrapolates to $p^\star$ for a large magnetic field, leading to a possible field dependence of the QCP (see also Ref. [44]). However, no indication for the presence of such a magnetic state in the vicinity of the onset of the pseudogap phase has been observed so far in Bi2201.

Finally, calculations for the two-dimensional Hubbard model in the doped Mott insulator regime [45] have proposed an alternative interpretation of these thermodynamic anomalies without invoking broken symmetries. A sharp crossover in the specific heat can occur when crossing the Widom line emanating from a finite-temperature critical endpoint of a first-order transition between a strongly correlated pseudogap phase (in which short-range antiferromagnetic correlations form singlet bonds) and a metal [46].

ACKNOWLEDGMENTS

The work in Grenoble was supported by the Laboratoire d'excellence LANEF (Grant No. ANR-10-LABX-51-01) and was performed at the LNCMI, a member of the European Magnetic Field Laboratory (EMFL). Work at the LNCMI was supported by the French Agence Nationale de la Recherche (ANR) (Contract No. ANR-19-CE30- 0019-01). L.T. acknowledges support from the Canadian Institute for Advanced Research (CIFAR) as a CIFAR Fellow and funding from the Institut Quantique, the Natural Sciences and Engineering Research Council of Canada (PIN:123817), the Fonds de Recherche du QuebecNature et Technologies (FRQNT), the Canada Foundation for Innovation (CFI), and a Canada Research Chair. This research was undertaken thanks, in part, to funding from the Canada First Research Excellence Fund and the Gordon and Betty Moore Foundation's EPiQS Initiative (Grant No. GBMF5306 to L.T.). J.C. acknowledge support from the Swiss National Science Foundation. We thank J.-M.S. Tramblay and C.M. Varma for fruitful discussions.

[1] D. C. Peets, J. D. F. Mottershead, B. Wu, I. S. Elfimov, R. Liang, W. N. Hardy, D. A. Bonn, M. Raudsepp, N. J. C. Ingle, and A. Damascelli, New J. Phys. **9**, 28 (2007).

[2] N. E. Hussey, M. Abdel-Jawad, A. Carrington, A. P. Mackenzie, and L. Balicas, Nature (London) **425**, 814 (2003).

[3] A. F. Bangura, P. M. C. Rourke, T. M. Benseman, M. Matusiak, J. R. Cooper, N. E. Hussey, and A. Carrington, Phys. Rev. B **82**, 140501(R) (2010).

[4] B. Michon, C. Girod, S. Badoux, J. Kacmarcik, Q. Ma, M. Dragomir, H. A. Dabkowska, B. D. Gaulin, J.-S. Zhou, S. Pyon, T. Takayama, H. Takagi, S. Verret, N. Doiron-Leyraud, C. Marcenat, L. Taillefer, and T. Klein, Nature (London) **567**, 218 (2019).

[5] S. Nakamae, K. Behnia, N. Mangkorntong, M. Nohara, H. Takagi, S. J. C. Yates, and N. E. Hussey, Phys. Rev. B **68**, 100502(R) (2003).

[6] Y. Wang, J. Yan, L. Shan, H.-H.. Wen, Y. Tanabe, T. Adachi, and Y. Koike, Phys. Rev. B **76**, 064512 (2007).

[7] K. Fujita, C. K. Kim, I. Lee, J. Lee, M. H. Hamidian, I. A. Firmo, S. Mukhopadhyay, H. Eisaki, S. Uchida, M. J. Lawler, E.-A. Kim, and J. C. Davis, Science **344**, 612 (2014).

[8] S. Badoux, W. Tabis, F. Laliberté, G. Grissonnanche, B. Vignolle, D. Vignolles, J. Beard, D. A. Bonn, W. N. Hardy, R. Liang, N. Doiron-Leyraud, L. Taillefer, and C. Proust, Nature (London) **531**, 210 (2016).

[9] C. Collignon, S. Badoux, S. A. A. Afshar, B. Michon, F. Laliberté, O. Cyr-Choinière, J.-S. Zhou, S. Licciardello, S. Wiedmann, N. Doiron-Leyraud, and L. Taillefer, Phys. Rev. B **95**, 224517 (2017).

[10] C. Putzke, S. Benhabib, W. Tabis, J. Ayres, Z. Wang, L. Malone, S. Licciardello, J. Lu, T. Kondo, T. Takeuchi, N. E. Hussey, J. R. Cooper, and A. Carrington, Nat. Phys. (2021), doi: 10.1038/s41567-021-01197-0.

[11] M. Lizaire, A. Legros, A. Gourgout, S. Benhabib, S. Badoux, F. Laliberté, M.-E. Boulanger, A. Ataei, G. Grissonnanche, D. LeBoeuf, S. Licciardello, S. Wiedmann, S. Ono, H. Raffy, S. Kawasaki, G.-Q. Zheng, N. Doiron-Leyraud, C. Proust, and L. Taillefer, arXiv:2008.13692.

[12] See for instance: H. V. Lohneysen, A. Rosch, M. Vojta, and P. Wolfle, Rev. Mod. Phys. **79**, 1015 (2007).

[13] N. Momono, M. Ido, T. Nakano, M. Oda, Y. Okajima, and K. Yamaya, Physica C **233**, 395 (1994).

[14] M. Frachet, I. Vinograd, R. Zhou, S. Benhabib, S. Wu, H. Mayaffre, S. Kramer, S. K. Ramakrishna, A. P. Reyes, J. Debray, T. Kurosawa, N. Momono, M. Oda, S. Komiya, S. Ono, M. Horio, J. Chang, C. Proust, D. LeBoeuf, and M-H. Julien, Nat. Phys. **16**, 1064 (2020).

[15] J. Chang, C. Niedermayer, R. Gilardi, N. B. Christensen, H. M. Rønnow, D. F. McMorrow, M. Ay, J. Stahn, O. Sobolev, A. Hiess, S. Pailhes, C. Baines, N. Momono, M. Oda, M. Ido, and J. Mesot, Phys. Rev. B **78**, 104525 (2008).

[16] S. Kawasaki, M. Ito, C. T. Lin, and G.-q. Zheng, J. Phys. Soc. Jpn (to be published).

[17] Y. Kohama *et al.*, Proc. Natl. Acad. Sci. USA **116**, 10686 (2019).

[18] Y. Wang and H.-H. Wen, Europhys. Lett. **81**, 57007 (2008).

[19] S. Komiya and I. Tsukada, J. Phys.: Conf. Ser. **150**, 052118 (2009).

[20] J. Chang, M. Shi, S. Pailhes, M. Meansson, T. Claesson, O. Tjernberg, A. Bendounan, Y. Sassa, L. Patthey, N. Momono, M. Oda, M. Ido, S. Guerrero, C. Mudry, and J. Mesot, Phys. Rev. B **78**, 205103 (2008).

[21] T. Yoshida, X. J. Zhou, K. Tanaka, W. L. Yang, Z. Hussain, Z.-X. Shen, A. Fujimori, S.Sahrakorpi, M. Lindroos, R. S. Markiewicz, A. Bansil, S. Komiya, Y. Ando, H. Eisaki, T. Kakeshita, and S. Uchida, Phys. Rev. B **74**, 224510 (2006).

[22] F. Laliberte, W. Tabis, S. Badoux, B. Vignolle, D. Destraz, N. Momono, T. Kurosawa, K. Yamada, H. Takagi, N. Doiron-Leyraud, C. Proust, and L. Taillefer, arXiv:1606.04491.

[23] G. S. Boebinger, Y. Ando, A. Passner, T. Kimura, M. Okuya, J. Shimoyama, K. Kishio, K. Tamasaku, N. Ichikawa, and S. Uchida, Phys. Rev. Lett. **77**, 5417 (1996).

[24] R. A. Cooper, Y. Wang, B. Vignolle, O. J. Lipscombe, S. M. Hayden, Y. Tanabe, T. Adachi, Y. Koike, M. Nohara, H. Takagi, C. Proust, and N. E. Hussey, Science **323**, 603 (2009).

[25] See Supplemental Material at http://link.aps.org/supplemental/10.1103/PhysRevB.103.214506 for the temperature dependence of the specific heat in all $La_{2-x}Sr_xCuO_4$ samples. It also includes further information on the field dependence at different temperatures in both $La_{2-x}Sr_xCuO_4$ and $Bi_{2+y}Sr_{2-x-y}La_xCuO_{6+\delta}$ as well as a comparison among the phonon, Schottky, and electronic contributions to the specific heat in both systems. Furthermore, it contains additional information on the way the Schottky contribution could be subtracted from the data in $Bi_{2+y}Sr_{2-x-y}La_xCuO_{6+\delta}$.

[26] B. Michon, A. Ataei, P. Bourgeois-Hope, C. Collignon, S. Y. Li, S. Badoux, A. Gourgout, F. Laliberté, J.-S. Zhou, N. Doiron-Leyraud, and L. Taillefer, Phys. Rev. X **8**, 041010 (2018).

[27] J. W. Loram, K. A. Mirza, W. Y. Liang, and J. Osborne, Physica C **162-164**, 498 (1989).

[28] T. Matsuzaki, N. Momono, M. Oda, and M. Ido, J. Phys. Soc. Jpn. **73**, 2232 (2004).

[29] M. Horio, K. Hauser, Y. Sassa, Z. Mingazheva, D. Sutter, K. Kramer, A. Cook, E. Nocerino, O. K. Forslund, O. Tjernberg, M. Kobayashi, A. Chikina, N. B. M. Schroter, J. A. Krieger, T. Schmitt, V. N. Strocov, S. Pyon, T. Takayama, H. Takagi, O. J. Lipscombe *et al.*, Phys. Rev. Lett. **121**, 077004 (2018).

[30] S. Kunisada, S. Isono, Y. Kohama, S. Sakai, C. Bareille, S. Sakuragi, R. Noguchi, K. Kurokawa, K. Kuroda, Y. Ishida, S. Adachi, R. Sekine, T. K. Kim, C. Cacho, S. Shin, T. Tohyama, K. Tokiwa, and T. Kondo, Science **369**, 833 (2020).

[31] Y. Ando, Y. Kurita, S. Komiya, S. Ono, and K. Segawa, Phys. Rev. Lett. **92**, 197001 (2004).

[32] J. G. Storey, Europhys. Lett. **113**, 27003 (2016).

[33] A. Eberlein, W. Metzner, S. Sachdev, and H. Yamase, Phys. Rev. Lett. **117**, 187001 (2016).

[34] S. Verret, O. Simard, M. Charlebois, D. Sénéchal, and A.-M. S. Tremblay, Phys. Rev. B **96**, 125139 (2017).

[35] S. Chatterjee and S. Sachdev, Phys. Rev. B **95**, 205133 (2017).

[36] Xiaoqing Zhou, D. C. Peets, Benjamin Morgan, W. A. Huttema, N. C. Murphy, E. Thewalt, C. J. S. Truncik, P. J. Turner, A. J. Koenig, J. R. Waldram, A. Hosseini, R. Liang, D. A. Bonn, W. N. Hardy, and D. M. Broun, Phys. Rev. Lett. **121**, 267004 (2018).

[37] T. Kondo, Y. Hamaya, A. D. Palczewski, T. Takeuchi, J. S. Wen, Z. J. Xu, G. Gu, J. Schmalian, and A. Kaminski, Nat. Phys. **7**, 21 (2011).

[38] S. Kawasaki, C. Lin, P. L. Kuhns, A. P. Reyes, and G.-q. Zheng, Phys. Rev. Lett. **105**, 137002 (2010).

[39] C. M. Varma, Rev. Mod. Phys. **92**, 031001 (2020).

[40] H. von Lohneysen, J. Phys.: Condens. Matter **8**, 9689 (1996).

[41] R. Daou, O. Cyr-Choinière, F. Laliberté, D. LeBoeuf, N. Doiron-Leyraud, J.-Q. Yan, J.-S. Zhou, J.-B. Goodenough and L. Taillefer, Phys. Rev. B **79**, 180505(R) (2009).

[42] F. Laliberté, J. Chang, N. Doiron-Leyraud, E. Hassinger, R. Daou1, M. Rondeau, B. J. Ramshaw, R. Liang, D. A. Bonn, W. N. Hardy, S. Pyon, T. Takayama, H. Takagi, I. Sheikin, L. Malone, C. Proust, K. Behnia, and L. Taillefer, Nat. Commun. **2**, 432 (2011).

[43] C. Proust and L. Taillefer, Annu. Rev. Condens. Matter Phys. **10**, 409 (2019).

[44] S. Sachdev, Phys. Status Solidi **247**, 537 (2010).

[45] G. Sordi, C. Walsh, P. Sémon, and A.-M. S. Tremblay, Phys. Rev. B **100**, 121105 (2019).

[46] G. Sordi, P. Semon, K. Haule, and A.-M. S. Tremblay, Sci. Rep. **2**, 547 (2012).